A specialized population of Periostin-expressing cardiac fibroblasts contributes to postnatal cardiomyocyte maturation and innervation

Luis Hortells[a], Iñigo Valiente-Alandi[a,b], Zachary M. Thomas[a], Emma J. Agnew[a], Dan J. Schnell[c], Allen J. York[a], Ronald J. Vagnozzi[a], Evan C. Meyer[d], Jeffery D. Molkentin[a], and Katherine E. Yutzey[a,1]

[a]The Heart Institute, Division of Molecular Cardiovascular Biology, Cincinnati Children's Hospital Medical Center, Department of Pediatrics, University of Cincinnati College of Medicine, Cincinnati, OH 45267; [b]Conservation Genetics, Institute for Conservation Research, San Diego Zoo, San Diego, CA 92101; [c]Division of Biomedical Informatics, Cincinnati Children's Hospital Medical Center, Cincinnati, OH 45229; and [d]The Confocal Imaging Core, Cincinnati Children's Hospital Medical Center, Cincinnati, OH 45229

Edited by Eric N. Olson, University of Texas Southwestern Medical Center, Dallas, TX, and approved July 24, 2020 (received for review May 8, 2020)

During the postnatal period in mammals, the cardiac muscle transitions from hyperplasic to hypertrophic growth, the extracellular matrix (ECM) undergoes remodeling, and the heart loses regenerative capacity. While ECM maturation and crosstalk between cardiac fibroblasts (CFs) and cardiomyocytes (CMs) have been implicated in neonatal heart development, not much is known about specialized fibroblast heterogeneity and function in the early postnatal period. In order to better understand CF functions in heart maturation and postnatal cardiomyocyte cell-cycle arrest, we have performed gene expression profiling and ablation of postnatal CF populations. Fibroblast lineages expressing Tcf21 or Periostin were traced in transgenic GFP reporter mice, and their biological functions and transitions during the postnatal period were examined in sorted cells using RNA sequencing. Highly proliferative Periostin (Postn)+ lineage CFs were found from postnatal day 1 (P1) to P11 but were not detected at P30, due to a repression of *Postn* gene expression. This population was less abundant and transcriptionally different from Tcf21+ resident CFs. The specialized Postn+ population preferentially expresses genes related to cell proliferation and neuronal development, while Tcf21+ CFs differentially express genes related to ECM maturation at P7 and immune crosstalk at P30. Ablation of the Postn+ CFs from P0 to P6 led to altered cardiac sympathetic nerve patterning and a reduction in binucleation and hypertrophic growth with increased fetal troponin (TroponinI1) expression in CM. Thus, postnatal CFs are heterogeneous and include a transient proliferative Postn+ population required for cardiac nerve development and cardiomyocyte maturation soon after birth.

cardiac fibroblast | postnatal heart | cardiomyocyte development | cardiac neuronal development | periostin

Heart disease is the dominant cause of death in the world (1), but there is still incomplete knowledge concerning the role and interactions of the different cell types present in the heart during development, maturation, and disease. During postnatal maturation in mice, heart muscle cells undergo significant changes including cell-cycle arrest, transition from hyperplasic to hypertrophic growth, and binucleation (2, 3). Several studies have focused on the differences between the postnatal and the adult heart response to injury (4), but there is still a gap in the knowledge of normal development of the heart soon after birth. Postnatal changes in the extracellular matrix (ECM) and their importance in cardiomyocyte maturation have been reported with increased matrix stiffness implicated in cardiomyocyte maturation (5, 6). Cardiac fibroblasts (CFs) are critical for ECM remodeling and homeostasis, but their specific roles in postnatal maturation of the heart and how the postnatal CF populations compare to adult CFs remain undefined. Here, we determine gene expression profiles of different postnatal cardiac fibroblast populations and examine their requirements in postnatal cardiac ECM formation, innervation, and cardiomyocyte (CM) maturation.

CFs in adult hearts are quiescent cells that derive mainly from epicardial progenitors during development (7–9). The main function attributed to CFs is the formation and remodeling of the ECM, which contributes to the architecture and contractile force of the heart (10). Functions of the ECM in CM proliferation have been described in regeneration (5) and embryonic development (11), but little is known about the crosstalk between CFs and CMs during postnatal maturation in vivo. In the postnatal heart, fibroblast diversity has been detected by single-cell analysis, but the specific functions and gene expression of these populations have not been defined (12). In the adult heart after injury, the resident quiescent CFs, lineage-traced by expression of transcription factor 21 (*Tcf21*) or platelet-derived growth factor receptor alpha (*PDGRFα*) (8, 9), become activated, and a specialized reparative subpopulation required for healing and scar formation expresses periostin (*Postn*) (13, 14). With pathologic ECM remodeling after injury, CFs additionally transdifferentiate into myofibroblasts which express alpha smooth muscle actin (αSMA) (8, 15, 16). Thus, diverse subpopulations of CFs contribute to homeostasis and disease with different levels of activation in response to cardiac insults. However, limited

Significance

During the postnatal period, the heart undergoes important changes, including cardiomyocyte cell-cycle arrest and loss of regenerative capacity. While other cell types have been better characterized, the information related to postnatal cardiac fibroblasts (CFs) is limited. Here, we report a specialized population of highly proliferative periostin-expressing (Postn+) fibroblasts in the early postnatal heart that become quiescent at P30. In comparison, P7 Tcf21+ fibroblasts have distinct gene expression from Postn+ CFs. Notably, Postn+ CFs express proliferation and neuronal-related genes, while Tcf21+ CFs preferentially express extracellular-matrix–related genes. Ablation of Postn+ cells leads to reduced cardiomyocyte growth, mitotic activity, and binucleation with increased sympathetic nerve area. Thus Postn+ cells represent a specialized developmental CF population critical for postnatal cardiac maturation.

Author contributions: L.H., J.D.M., and K.E.Y. designed research; L.H., I.V.-A., Z.M.T., E.J.A., A.J.Y., R.J.V., and E.C.M. performed research; L.H., I.V.-A., D.J.S., A.J.Y., R.J.V., E.C.M., J.D.M., and K.E.Y. analyzed data; and L.H., J.D.M., and K.E.Y. wrote the paper.

The authors declare no competing interest.

This article is a PNAS Direct Submission.

[1]To whom correspondence may be addressed. Email: katherine.yutzey@cchmc.org.

This article contains supporting information online at https://www.pnas.org/lookup/suppl/doi:10.1073/pnas.2009119117/-/DCSupplemental.

First published August 17, 2020.

information is available on neonatal CF diversity or specific functions of CF populations in the period after birth.

During the postnatal period, the heart undergoes maturation in response to increased cardiac demand and growth, while losing regenerative capacity. In addition, the cardiac ECM undergoes significant remodeling with increased stiffness (5, 6). At the same time, rodent CMs undergo binucleation and cell-cycle arrest during the first week after birth (17) with a transition from hyperplasic to hypertrophic CM growth (2, 18). Moreover, CMs undergo metabolic maturation and induction of adult sarcomeric protein isoforms (19) in the first two postnatal weeks (20). Similarly, cardiac innervation and patterning on the heart surface becomes more complex during the first month after birth (21). The specific contributions of CFs to neonatal heart maturation, notably through crosstalk with other cells including cardiomyocytes and nerves, remain largely unknown.

The specific roles of heterogeneous populations of CFs in the postnatal heart are not well characterized. In the present work, we study the diversity of CF populations during postnatal development when the ECM of the heart is undergoing dynamic remodeling (22). In addition, through ablation studies in vivo, we demonstrate that, during the first week after birth, Postn+ lineage CFs are required for normal heart maturation.

Results

Postnatal Cardiac ECM Maturation Includes Reduction of Cardiac Fibronectin and Increased Fibrillar Collagen Remodeling in the Week after Birth. A primary function of cardiac fibroblasts is the production of ECM, which undergoes dynamic changes during postnatal development.

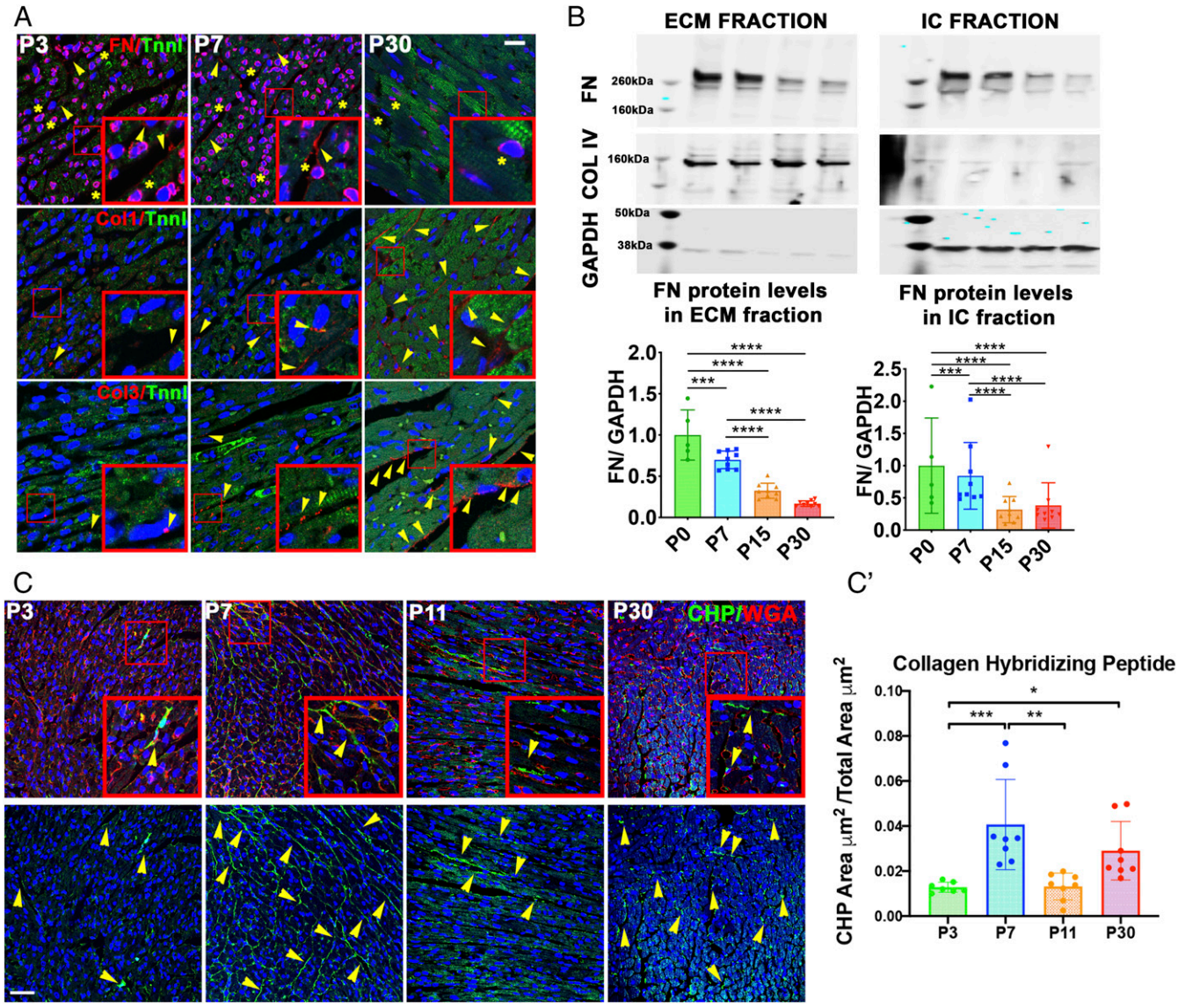

Fig. 1. The cardiac extracellular matrix is remodeled from P0 to P30. (*A*) At P3, P7, and P30, the left ventricle free wall shows loss of Fn but gain of Col1 and Col3 from P0 to P30 as indicated by immunofluorescence (red). Cardiomyocytes were immunostained using TnnI (green). Extracellular protein expression is indicated by yellow arrowheads, while stars mark intracellular expression of the proteins. (Scale bar: 10 μm.) Images are representative of $n = 4$. Small red boxes indicate the original area of the *Insets*. (*B*) P0, P7, P15, and P30 Western blot of ventricular protein from the ECM and the intracellular (IC) fractions normalized to intracellular GAPDH expression show a progressive loss of expression of Fn from P0 to P30. Col IV was used as loading control for the ECM fraction. The absence of GAPDH in the ECM fraction and Col IV in the IC fraction confirm the purity of the separations. $n = 5$. (*C*) Fibrillar collagen remodeling in P0, P7, P11 and P30 left ventricular free wall is shown by Fluorescein-Collagen Hybridizing Peptide/Wheat Germ Agglutinin (WGA) staining (yellow arrowheads). (Scale bar: 20 μm.) (*C'*) Remodeling collagen was quantified from *C* as the ratio of area of CHP reactivity per total tissue area showing dynamic collagen remodeling from P3 to P30. $n = 8$. DAPI was used to stain the nuclei. ****$P < 0.0001$, ***$P < 0.001$, **$P < 0.01$, and *$P < 0.05$ by Kruskall–Wallis tests.

The expression of fibronectin (Fn), indicative of immature ECM and implicated in late fetal CM proliferation (11), was compared to mature collagen expression and remodeling as a measure of ECM maturation in the postnatal period (22). Fn was highly expressed at P3 and P7 (Fig. 1*A*), but this expression was reduced by P30 in both the extracellular (arrowheads in Fig. 1*A*) and intracellular areas (stars in Fig. 1*A*) of, not only CFs, but also CMs. Myocardial expression of Fn, as quantified by Western blot, is reduced in the extracellular and intracellular fractions at P30 (Fig. 1*B*). In contrast, the major fibrillar collagens (Col1 and Col3) are weakly expressed at P3 but are present adjacent to maturing CMs at P7 and P30. Likewise, levels of collagen remodeling, detected

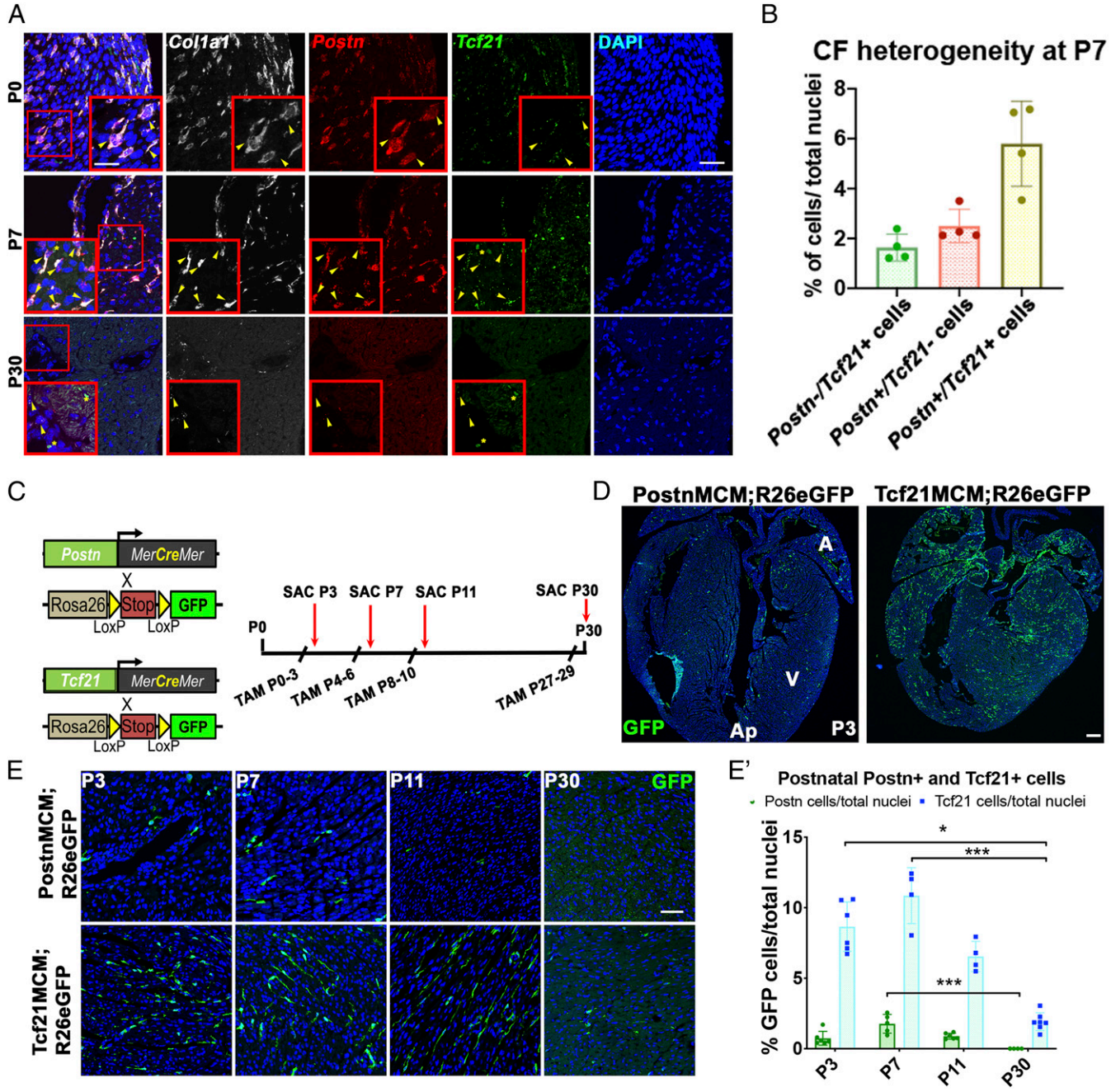

Fig. 2. Postn+ CFs are present in the postnatal heart. (*A*) P0, P7, and P30 RNAscope of *Col1a1*, *Postn*, and *Tcf21* (yellow arrowheads) shows positive colocalization of *Postn*, *Tcf21*, and *Col1* confirming the fibroblast identity of these cells. (Scale bar: 10 μm.) Yellow stars mark blood cell autofluorescence. (Scale bar, *Inset*: 2.5 μm.) (*B*) Cell counting from RNAscope staining of the left ventricular free wall shows three different populations expressing *Postn*, *Tcf21*, or both. The most prevalent population found was the one coexpressing *Tcf21* and *Postn*. $n = 4$. An average of 7,700 nuclei were counted per biological replicate. (*C*) Diagram of the genetic models and time points used for lineage tracing of Tcf21+ and Postn+ cells. (*D*) GFP+ cell localization in $Tcf21^{MCM};R26^{eGFP}$ and $Postn^{MCM};R26^{eGFP}$ hearts at P3. (Scale bar: 100 μm.) (*E*) P3, P7, P11, and P30 immunofluorescence of GFP in $Postn^{MCM};R26^{eGFP}$ and $Tcf21^{MCM};R26^{eGFP}$ mice. (Scale bar: 50 μm.) (*E'*) Cell counts of GFP+ normalized to total DAPI-stained nuclei per area from *E* revealed five times more Tcf21+ cells than Postn+ cells up to P11, with no detectable Postn+ cells at P30. $n = 4$ to 7. An average of 40,000 cells from the left ventricle were counted per biological replicate. DAPI was used to stain the nuclei. ***$P < 0.001$, *$P < 0.05$ by Kruskall–Wallis test. For *E'*, independent Kruskall–Wallis tests were run independently for Postn+ and for Tcf21+ cells.

using a collagen hybridizing peptide (CHP) (Fig. 1*C*), increase from P3 to P30. Together these data show that the cardiac ECM transitions from abundant Fn to predominantly fibrillar collagen in the postnatal period in mice with significant ECM changes taking place between birth and P7.

Heterogeneous Populations of Postn+ and Tcf21+ Expressing CFs Are Present in the Postnatal Heart. CFs become activated when intensive ECM production and remodeling are required both during development and after injury (8). Since ECM remodeling is active during the postnatal period, the presence of specialized

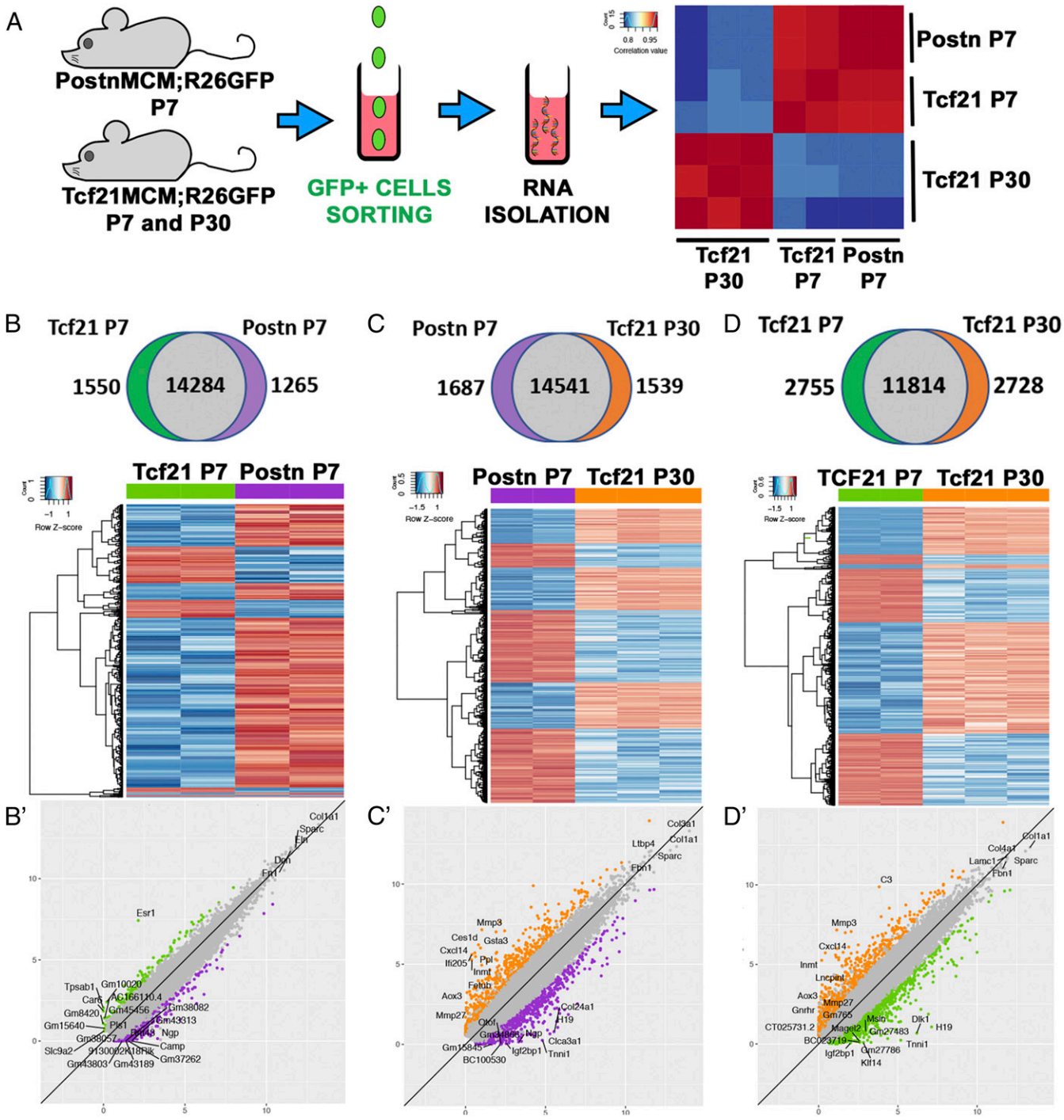

Fig. 3. Transcriptome analysis of P7 Postn+, TCF21+ CFs, and P30 TCF21+ CFs unveils population heterogeneity at P7 and changes in the different CFs expression from P7 to P30. (*A*) Diagram showing the animal models and the protocol for RNAseq analysis. (*B–D*) Venn diagrams and heatmaps of the differentially expressed genes of Postn+ P7, Tcf21+ P7, and Tcf21+ P30 cell fractions show different transcriptomes for the three populations sorted (purple: Postn+ P7; green: Tcf21+ P7; and orange: Tcf21+ P30). (*B′–D′*) Scatter plots of the transcriptome of different CFs: purple: Postn+ P7; green: Tcf21+ P7; and orange: Tcf21+ P30; and common genes: gray. The scatter plots show that the three populations express typical CF markers, but they also present differential expression of nonfibroblastic genes. The genes showed in the graph are the top 10 differentially expressed genes, and the common genes shown are typical ECM CF markers.

populations of activated CFs was evaluated by examining *Postn* gene expression. In the injured heart, Postn is a marker of reparative CFs that later turn into pathologic myofibroblasts that express αSMA (14, 15). RNA expression in individual cells was assessed with RNAscope in situ hybridization (Fig. 2*A*), which demonstrates that *Postn*-expressing cells also express *Col1a1* and, in a majority of cases, *Tcf21*, supporting their CF identity. Notably *Postn*-expressing CFs were detected at P0 and P7 during active ECM remodeling and cardiomyocyte maturation, but not at P30. At P7, ∼6% of the total nuclei in the heart coexpressed *Tcf21* and *Postn*, while 2% expressed each gene independently (Fig. 2*B*). Thus, CFs are heterogeneous. In addition, overall transcript levels of all of the genes examined were reduced at P30, consistent with CF quiescence at this stage. To confirm the fibroblast identity of *Tcf21*-expressing cells, *Tcf21* RNA expression was compared to *TroponinT2* (cardiomyocyte marker) and *CD31* (PECAM, endothelial marker) (*SI Appendix*, Fig. S1*A*) by RNAscope. As expected, *Tcf21* expression was not detected in cardiomyocytes or endothelial cells, confirming the specificity of *Tcf21* as a CF-lineage marker. Therefore, CFs present during the P0-to-P30 postnatal period differentially express *Postn* and/or *Tcf21*. In addition, maturation of CF populations is indicated by reduced *Postn* expression after P7.

In order to compare Postn+ and Tcf21+ expressing lineages of CFs at specific time points, offspring from GFP reporter mice bred to gene-targeted mice with Postn or Tcf21-specific tamoxifen (TAM)-inducible Cre expression were analyzed in the postnatal period. Postn+ CFs were identified using TAM-inducible $Postn^{MCM/+}$;$R26^{eGFP}$ mice compared to Tcf21+ cell lineage analysis of resident CFs in $Tcf21^{MCM/+}$;$R26^{eGFP}$ animals (Fig. 2*C*). Mice were injected with TAM (10 mg/kg) 3 d before harvesting the hearts at P3, P7, P11, and P30 in order to determine the number of cells and their location in the heart at specific time intervals during the postnatal period. The Postn+ CFs were detected by GFP expression in the left ventricle up to P11, while the Tcf21+ CFs were present through the postnatal period to P30 (Fig. 2*E*). At P3, both populations were visually more prevalent in the atria and the base of the ventricles (close to the heart valves) than in the apex (Fig. 2*D*). When counted, the numbers of Tcf21+ CFs in the left ventricle were 5× higher than the Postn+ CFs in the same location (Fig. 2*E*). Interestingly, the number of Postn+ CFs obtained by lineage tracing was smaller than the number of cells expressing *Postn* messenger RNA (mRNA) as indicated by RNAscope (2% vs. 6 to 8%, respectively), which is likely due to the expression threshold required to activate the Cre-dependent GFP reporter gene. To confirm the fibroblast identity of the traced cells, GFP expression was analyzed with CD31 (PECAM) and CD45 (marker immune cells). Neither CD31 nor CD45 markers were coexpressed with GFP+ in Tcf21+ or Postn+ lineages, further confirming the specificity of the CF lineage tracing (*SI Appendix*, Fig. S1 *B* and *C*). Importantly, coexpression of the activated myofibroblast marker αSMA with GFP in the $Postn^{MCM/+}$;$R26^{eGFP}$ and $Tcf21^{MCM/+}$;$R26^{eGFP}$ hearts was not detected at P7 (8, 15, 16), which differentiates the Postn+ CFs from pathological myofibroblasts.

The efficiency of lineage tracing and potential overlap in the genetically traced Postn+ and Tcf21+ populations were assessed by RNAscope. *Postn* and *Tcf21* gene expression was compared to *eGFP* RNA expression to compare endogenous gene expression with the GFP lineage reporter (*SI Appendix*, Fig. S2 *A* and *B*, respectively). Only 19% of the cells expressing *Postn* were also positive for *eGFP* in the $Postn^{MCM}$;$R26^{eGFP}$ mice (*SI Appendix*, Fig. S2*A*′). Alternatively, in the $Tcf21^{MCM}$;$R26^{eGFP}$ lineage-traced hearts, the *Tcf21*+/*eGFP*+ cells were 60% of the total *Tcf21*-expressing cells (*SI Appendix*, Fig. S2*B*′). Interestingly, 99% of the *Tcf21*/*eGFP*+ cells were also positive for *Postn* in the $Tcf21^{MCM}$;$R26^{eGFP}$ hearts (Fig. 2*B*″). Conversely, in the $Postn^{MCM}$;$R26^{eGFP}$ hearts only 45% of the *Postn*+/*eGFP*+ cells were also *Tcf21*+ (*SI Appendix*, Fig. S2*A*″). At P30, Postn+ CFs with TAM induction at P0 to P4 maintain expression of *eGFP* mRNA (*SI Appendix*, Fig. S2*C*), but only a small fraction (7%) of the *eGFP*+ cells weakly express endogenous *Postn*. Moreover, 50% of the *eGFP*+ cells express *Tcf21*, which is a similar fraction of the cells with coexpression at P7 (*SI Appendix*, Fig. S2*D*). Thus, at P7 the Postn+ lineage CFs marked by $Postn^{MCM}$;$R26^{eGFP}$ represent a subfraction of the *Postn*-expressing cells, and there is partial overlap in endogenous *Tcf21* and *Postn* expression. In addition, at P30, *Postn* expression is down-regulated, but *Tcf21* expression is maintained in the Postn+ CF lineage.

Postn+ and Tcf21+ Cardiac Fibroblast Lineages Have Different Gene Expression Profiles. To interrogate gene expression profiles for Postn+ and Tcf21+ CF lineages during postnatal heart maturation, Postn+ and Tcf21+ CF populations were isolated based on GFP expression at P7 after TAM induction at P4 to P6. Postn+ and Tcf21+ lineage fibroblasts involved in myocardial maturation active at P7 were compared to the more mature and quiescent Tcf21+ CFs with TAM induction at P27 to P29. Since the number of Postn+ lineage cells decline after P7 and they are undetectable with TAM induction at P27 to P29, P30 Postn+ CFs are not available for analysis. The GFP+ cells from ventricular tissue were isolated by fluorescence activated cell sorting. The RNA from the sorted GFP+ cells was isolated, subjected to RNA sequencing (RNA-seq), and gene expression profiles were analyzed (Fig. 3*A*). The expression profiles of the three populations were compared as Postn+P7 vs. Tcf21+P7 (Dataset S1), Postn+P7 vs. Tcf21+P30 (Dataset S2), and Tcf21+P7 vs. Tcf21+P30 (Dataset S3). The most extensive differences in gene expression were observed between Tcf21+ CFs at P7 and Tcf21+ CFs at P30 (with a minimum of 2,728 differentially expressed genes). Fewer differences in gene expression were observed between Postn+ P7 CFs and Tcf21+ P7 CFs (with a minimum of 1,265 differentially expressed genes) (Fig. 3 *B*–*D*). The expression of the majority of the genes was not different between the Postn+ and Tcf21+ CFs at P7; however, significant differences in subsets of genes were observed.

As expected, among the genes expressed in all three populations were CF typical genes, such as *Col1*, *Col3*, *Col4*, *Fbn1*, and *SPARC* (Fig. 3 *B*′–*D*′), corroborating the fibroblast identity of the GFP+ cells. However, differential expression of ECM genes in Tcf21+ CFs was observed with increased expression of *Col24a1*, *Adamts17*, *Emilin3*, *Tnc*, and also *Fn1* (confirming the results from Fig. 1 *A* and *B*) at P7 and with increased matrix-remodeling enzyme genes *Mmp3* and *Mmp27* at P30. From the differentially expressed gene lists (Datasets S2 and S3), it is interesting to note that both Postn+ and Tcf21+ CFs at P7 expressed more *H19*, an imprinted gene related to Igf2 regulation of cell proliferation and organ size, than Tcf21+ CFs at P30 (Fig. 3 *C*′ and *D*′). However, only Tcf21+ had higher expression of the imprinted gene *Dlk1*, which has been recently shown to inhibit CF proliferation and activation (23) (Fig. 3*D*′). When Dlk1 and GFP expression was assessed, the number of the CFs expressing Dlk1 at the protein level supported the RNA-seq findings, with greater expression in the Tcf21+ CFs at P7, than in the Postn+ CFs at P7, and with the lowest expression in the Tcf21+ CFs at P30 (*SI Appendix*, Fig. S3). A potentially important gene with higher expression in both Postn+P7 and TCF21+P7 CFs, compared to Tcf21+P30 CFs, was *Igf2bp1*, since other Igf-binding proteins were recently reported to promote CM proliferation and cardiac regeneration capacity (24). On the other hand, the P30 Tcf21+ CFs displayed higher expression of *Mmp3*, *Cxcl14*, and *C3* (Fig. 3 *C*′ and *D*′) in agreement with a final ECM-remodeling step in the postnatal period and immune crosstalk functions. Together, the gene expression profiles of the sorted CF lineages suggest that Postn+ and Tcf21+ lineage cells represent different CF populations at P7, with both having differences in

gene expression from the mature quiescent P30 Tcf21+ CFs. These results demonstrate the heterogeneity, as well as the maturation, of CFs during the postnatal period.

Postn+ CFs Have Enhanced Proliferation and Neuronal Development Functions at P7, While Tcf21+ CFs Preferentially Express Genes Related to ECM Functions at P7 and Immune Crosstalk at P30. Biological functions of differentially expressed genes in Postn+P7, Tcf21+P7, and Tcf21+P30 CF populations were identified by gene ontology (GO) term analysis (Dataset S4). The main biological functions of Postn+P7 CFs were related to cell division, when compared to Tcf21+P30, and to neuronal development, when compared to Tcf21+P7. To corroborate these functions, confirmation of the biological processes related to cell proliferation (Fig. 4*A*) were conducted using PH3+ and Ki67+ protein immunostaining in GFP+ cells from *Postn*$^{MCM/+}$;*R26*^{eGFP} and *Tcf21*$^{MCM/+}$;*R26*^{eGFP} left ventricles (Fig. 4 *B* and *C*). Increased numbers of PH3+/GFP+ cells were present in Postn+ and Tcf21+ populations at P3 and P7, in comparison to Tcf21+ CFs at P30. Moreover, the proliferative index in the Postn+ cells is higher than the Tcf21+ CFs at P3 and P7 (Fig. 4*C′*). In agreement with a more quiescent status of the CFs, PH3+/GFP+ cells were undetectable at P30 (Fig. 4*C′*). Therefore, Postn+ CFs have an increased proliferation rate compared to TCF21+ at P7, and both populations reduce their cell cycling after P7, becoming quiescent by P30.

Comparison of Postn+P7 and Tcf21+P7 CFs demonstrated enriched neuronal-related biological functions, including expression of neuronal differentiation-related genes in Postn+ cells (*SI Appendix*, Fig. S4*A*). Immunofluorescence and confocal microscopy were used to demonstrate that Postn+ cells are localized in proximity to neurons indicated by tyrosine hydroxylase (TH) expression at P7 (*SI Appendix*, Fig. S4*B*). In addition, a subset of Postn+ cells was also found in contact with the neuron-associated Schwann cell marker neuronal growth factor receptor (12, 25) (*SI Appendix*, Fig. S4*C*). Furthermore, ligands differentially expressed in the Postn+P7 CFs were implicated in neuronal signaling (*Ntng1*, *Npff*, *Bcan*, *Bdnf*, and *Nlgn1*), and the expression of *Bdnf* by Postn+ cells was confirmed by RNAscope (*SI Appendix*, Fig. S4*D*), supporting potential Postn+ CF-neuronal crosstalk in the early postnatal period. On the other hand, Tcf21+ CFs at P7 exhibited important ECM-related functions (*SI Appendix*, Fig. S5), while at P30 the Tcf21+ CFs exhibited immune crosstalk gene expression (*SI Appendix*, Fig. S6).

Additional cell–cell crosstalk mechanisms were examined by analysis of secreted protein gene expression in Postn+P7 vs. Tcf21+P7 CFs, as well as in Tcf21+P7 vs. Tcf21+P30 CFs

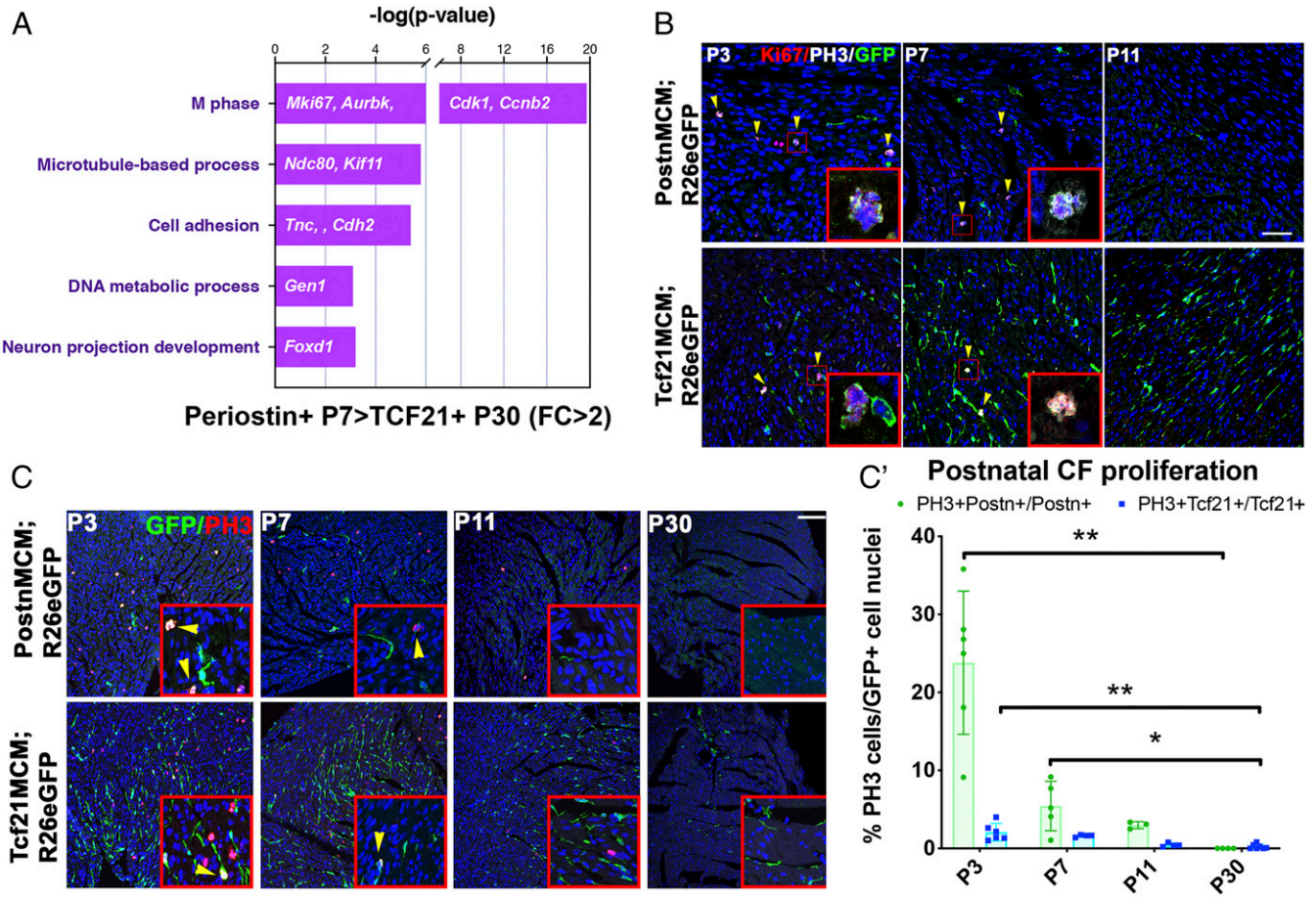

Fig. 4. The Postn+ CFs have higher cell-cycling activity than the Tcf21+ CFs from P0 to P7, and the Tcf21+ CFs are mitotically quiescent at P30. (*A*) DAVID pathways enriched in P7 Postn+ ventricular cells compared with Tcf21+ P30 CFs show biological functions related to cell proliferation. A number of differentially expressed genes are shown; the *x*-axis shows −log10 *P* values. FC: Fold Change. (*B*) P3, P7, and P11 *Postn*^{MCM};*R26*^{eGFP} and *Tcf21*^{MCM};*R26*^{eGFP} left ventricle immunofluorescence of Ki67, PH3, and GFP showing CF cell cycling in GFP+ cells (yellow arrowheads) up to P7. Higher magnification *Insets* show cells with PH3/MKi67 and GFP expression. (Scale bar: 50 μm.) DAPI was used to stain the nuclei. Kruskall–Wallis tests were run independently for Postn+ and for Tcf21+ cells. (*C*) P3, P7, P11, and P30 *Postn*^{MCM};*R26*^{eGFP} and *Tcf21*^{MCM};*R26*^{eGFP} left ventricle immunofluorescence of PH3 and GFP. (*C′*) Cell count from *A* shows higher Postn+/PH3+ CFs than Tcf21+/PH3 CFs up to P7, and reduced cycling activity of CFs at P30. (Scale bar: 50 μm.) $n = 4$ to 7. $^{**}P < 0.01$, $^{*}P < 0.05$ by Kruskall–Wallis test. An average of 40,000 cells were counted per biological replicate.

(*SI Appendix*, Fig. S7). The secreted protein genes with enhanced expression in Tcf21+P7 cells include *Igf2*, *Igf2bp1*, and *Tnc*, which are implicated in myocardial growth. In contrast, Postn+P7 cells have an enhancement of secreted ligands important for neurogenesis (*Ntng1*, *Bdnf*, *Nlgn1*, and *Npff*). Other secreted protein genes with enhanced expression in Postn+P7 vs. Tcf21+P7 cells include differentiation and growth-related ligands (*Ltf*, *Egf*, *Adam28*, *S100A8*, and *BMP5*), while innate immune-related genes were enhanced in Tcf21+P7 vs. Postn+P7 cells. Thus, the secreted protein gene profiles that increased in Tcf21+P7 compared to Tcf21+P30 CFs and in Postn+ compared to Tcf21+ CF at P7 include important ligands related to CM proliferation and support a role for cardiac fibroblasts in postnatal cardiomyocyte maturation in the week after birth.

Ablation of the Tcf21+ CFs and Postn+ CFs from P0 to P7. To study the consequences of CF depletion during the first week after birth in the mouse, Postn+ and Tcf21+ populations were ablated independently using a $R26^{DTA}$ gene for Cre-dependent tamoxifen-inducible expression of diphtheria toxin antigen (*SI Appendix*, Fig. S8*A*). We performed intragastric TAM injections (10 mg/kg) from P0 to P6 and harvested the hearts at P7. The fficacy of the ablation was confirmed by cell death detection with terminal deoxynucleotidyl transferase dUTP nick end labeling (TUNEL) and by quantification of the reduction of *Postn*- and *Tcf21*-expressing CFs using RNAscope. As an independent assessment of loss of the $Postn^{MCM};R26^{DTA}$ and $Tcf21^{MCM};R26^{DTA}$ recombined cells, the number of GFP+ cells was determined in mice with a Cre-dependent $R26^{mTmG}$ reporter gene (green in recombined cells) (*SI Appendix*, Fig. S8). Efficient ablation of CFs was apparent by the significantly reduced number of GFP+ cells compared to the negative controls. The specificity of the ablation and lack of an immune response was demonstrated by no change in the numbers or proliferation of CD45+ immune cells (*SI Appendix*, Fig. S8*D*), CD31+ endothelial cells, or αSMA+ vascular smooth muscle cells (*SI Appendix*, Fig. S9). The effect of ablation of Postn+P7 cells on overall cardiac and systemic growth was examined. While TUNEL+ cells were observed in thyroid glands of $Postn^{MCM}R26^{DTA}$ mice at P7, no differences in blood serum thyroxine were detected. In addition, no differences in heart or body weights were observed, and animals were overtly normal at P7 (*SI Appendix*, Fig. S10). Therefore, this approach leads to effective ablation of Postn+ and Tcf21+ CF populations after birth.

Importantly, due to the ECM-remodeling role of the CFs, collagen remodeling detected by CHP staining was assessed after CF ablation. While no significant changes were found after Postn+ CF ablation (*SI Appendix*, Fig. S11 *A* and *A′*), collagen remodeling was significantly reduced at P7 after Tcf21+ ablation (*SI Appendix*, Fig. S11 *B* and *B′*). No differences in Col1 expression were found (*SI Appendix*, Fig. S11 *A″* and *B″*), but this could be due to the relatively low amount of Col1 detected in P7 hearts. The reduced collagen remodeling found after Tcf21+ lineage ablation supports the idea that Tcf21+ CFs function in postnatal ECM-related processes, in agreement with the GO analysis of differential gene expression in Tcf21+ CFs from RNAseq (*SI Appendix*, Fig. S5*A*).

From P0 to P7, the Postn+ Lineage CFs Contribute to Cardiac Nerve Maturation. The crosstalk between CFs, neurons, and glial cells has not been previously addressed, and the role of CFs in postnatal maturation of the cardiac neurons has not been characterized previously. Postn+ CFs express neurodevelopment ligand genes and are located adjacent to developing neurons at P7 (*SI Appendix*, Fig. S4); thus, the effect of the ablation of Postn+ and Tcf21+ CFs on neuronal development was studied. Sympathetic neurons were identified by TH immunofluorescence (Fig. 5 *A* and *B*), and the area of positive signal was increased after Postn+ CF ablation, but not when Tcf21+ CFs were ablated. The three-dimensional (3D) patterning of cardiac innervation was interrogated by fluorescence whole-mount staining (Fig. 5*C*). An increased sympathetic nerve area was detected after ablation of Postn+ CFs at P7, but the total number of branching events was not significantly altered. Finally, to assess if the increased neuronal area affected normal heart conduction, electrocardiograms (ECGs) were performed on control and Postn+ CF-ablated P7 pups (Fig. 5*D* and *SI Appendix*, Fig. S12). Interestingly, a deeper Q wave was detected in the QRS complex of the Postn+ CF-ablated hearts. In humans this event is related to an abnormal ventricular conduction, but it is unclear if this could be extrapolated to experimental animal models. Together, these results suggest a possible role of Postn+ CFs in postnatal sympathetic nerve maturation, potentially related to growth of the sympathetic nerves.

Ablation of Postn+ CFs from P0 to P7 Interferes with Normal Cardiomyocyte Growth, Binucleation, and the Immature TroponinI1 Isoform Expression. The effects of Tcf21+ and Postn+ CF ablation on cardiomyocyte cell-cycle arrest and maturation were examined. While ablation of Tcf21+ CFs did not significantly affect cardiomyocyte mitotic activity, the percentage of PH3+ cardiomyocytes decreased after the ablation of the Postn+ CFs (Fig. 6 *A′* and *B′* and *SI Appendix*, Fig. S13*A*), suggesting a direct effect of Postn+ CFs on cardiomyocyte cell cycling. However, cytokinesis as indicated by ABK expression was unchanged (Fig. 6 *C* and *C′*), pointing to a reduction in nuclear division while cytokinesis remained unaltered. We also studied a possible enrichment of the Postn+ CFs near PH3+ CMs in P7 $Postn^{MCM/+};R26^{eGFP}$ (*SI Appendix*, Fig. S13*B*) and $Tcf21^{MCM/+};R26^{eGFP}$ hearts. The Postn+ CFs were found 4× more likely to be in proximity to cycling CMs than Tcf21+ CFs (*SI Appendix*, Fig. S13*B′*), and 40% of the PH3+ CMs were located close to Postn+ CFs (*SI Appendix*, Fig. S13*B″*). Since cardiomyocyte mitotic activity decreased with ablation of Postn+ CF, nucleation of CMs was examined in dissociated P7 control and Postn+ CF-ablated hearts (Fig. 6*D*). As expected, 70% of cardiomyocytes were binucleated in controls, but the presence of binucleated CMs was significantly decreased in Postn+ ablated hearts to 50% (Fig. 6*D′*). Dissociated cardiomyocyte size also was reduced after Postn+ CF ablation (Fig. 6*D″*). However, the total number of CMs per ventricle was not significantly altered in the Postn+-ablated hearts relative to controls (Fig. 6*D‴*). Together, these data suggest that the ablation of Postn+ CFs from P0 to P7 interferes with normal CM mitotic activity, binucleation, and growth.

Measurements of the cross-sectional area of Desmin+ cardiomyocytes demonstrated a decrease in CM size with ablation of Postn+ cells in vivo (Fig. 6 *E* and *E′*). One of the characteristics of postnatal CM maturation is the down-regulation of fetal sarcomeric protein genes including *Troponin I 1* (*TnnI1*). In the Postn+ CF-ablated hearts, increased expression of TnnI1 in the CMs was observed by immunofluorescence (Fig. 6*F*) and RNA expression (Fig. 6*G*) in the Postn+ CF-ablated hearts. On the other hand, no changes were detected in RNA expression of other markers of CM maturation including *TnnI3*, *Myh6*, *Myh7*, *Acadm*, and *Cpt2* (*SI Appendix*, Fig. S13*C*). Immunofluorescence assessment of T-tubule architecture and expression by MG29/Desmin did not showed any major differences after Postn+ CF ablation (*SI Appendix*, Fig. S13*D*). Moreover, no changes in heart weight (*SI Appendix*, Fig. 14 *A–C*) or functionality based on echocardiographic studies (*SI Appendix*, Fig. 14 *D–H*) were observed. Together, these data show that Postn+ CFs are required from P0 to P7 for normal CM binucleation, hypertrophic growth, and down-regulation of the immature sarcomere protein TnnI1.

Discussion

Here, we report different populations of CFs present in the postnatal heart with critical functions in cardiac organogenesis. These studies demonstrate for the first time a heterogeneous specialized population of CFs with transient Postn expression in

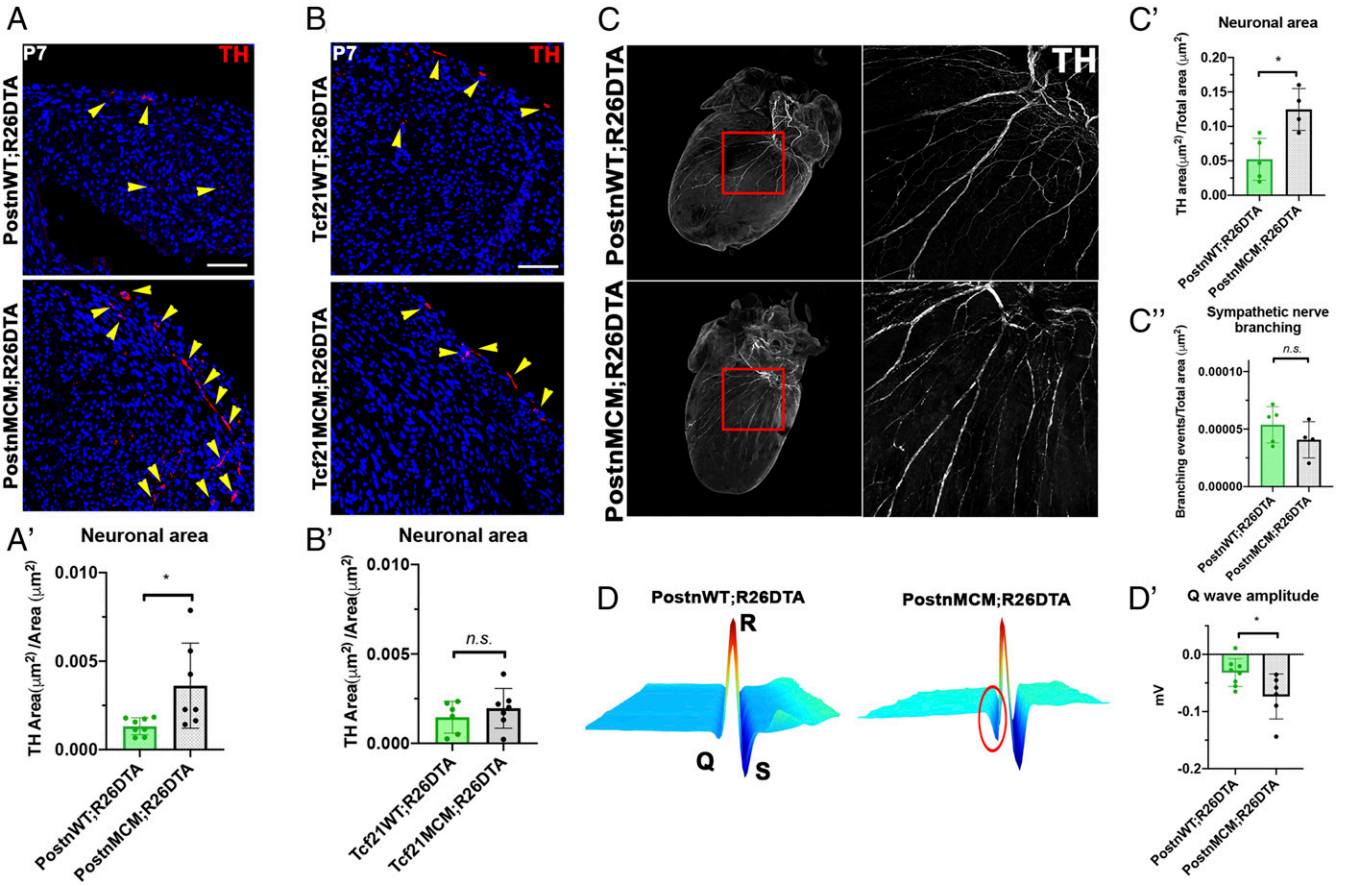

Fig. 5. The ablation of Postn+ CFs induces changes in postnatal cardiac neuronal remodeling. (*A* and *B*) *Postn*^{MCM};*R26*^{DTA} and control *Postn*^{WT};*R26*^{DTA} and *Tcf21*^{MCM};*R26*^{DTA} and control *Tcf21*^{WT};*R26*^{DTA} left ventricle TH immunostaining at P7. (Scale bar: 50 μm.) (*A′* and *B′*) TH was quantified from *A* and *B* as the ratio of area of TH reactivity per total tissue area, showing increased neuronal surface after Postn+ CF ablation but not after Tcf21+ CF ablation. $n = 6$ to 8. (*C*) Whole-mount heart immunostaining was used to measure total neuronal surface and number of branching events. (*C′*) Quantification of branching events reveals increased nerve area after Postn+ CF ablation. $n = 4$ to 5. (*C″*) No significant changes in nerve branching were detected after Postn CF ablation. $n = 4$ to 5. (*D*) Waterfall plots of the QRS obtained from *Postn*^{MCM};*R26*^{DTA} and control *Postn*^{WT};*R26*^{DTA} ECG analysis. A deeper Q wave (red circle) can be seen after Postn+ CF ablation. (*D′*) Quantification of the Q wave amplitude reveals a significantly deeper Q wave in the Postn+ CF-ablated hearts. (Scale bar: 50 μm.) $n = 4$. DAPI was used to stain the nuclei. *$P < 0.05$, n.s., not significant by Mann–Whitney test.

the normal postnatal heart that contributes to early CM maturation and sympathetic innervation after birth.

During the postnatal period, critical changes in ECM structure and composition are necessary to meet increased cardiac demands after birth (6, 26). A fibronectin-enriched ECM at P7 transitions into a more mature and fibrillar collagen-rich ECM at P30 (5). This transition has been implicated in the transition from cardiac regeneration to fibrotic response after injury, with higher expression of Fn in regenerative animals including the zebrafish (5). P7 seems to be a critical point for this transition, since deposition of Col1 and 3 (fibrillar collagens) and collagen-hybridizing peptide reactivity peak at this stage. This production of a stiffer collagen-rich ECM occurs with similar timing to the loss of cardiac regenerative capacity and the transition of cardiomyocytes from hyperplastic to hypertrophic growth (5, 6). Interestingly, a similar pattern in collagen remodeling has recently been detected by collagen-hybridizing peptide in neonatal pigs (27). With important ECM changes, the early postnatal period represents a critical period of fibroblast activity in the postnatal heart.

In adult hearts, cardiac fibroblasts are considered to be quiescent with low proliferation and turnover of ECM (7, 8). When important ECM remodeling is required, for example, after myocardial infarction, a specialized subpopulation of CFs becomes activated, expresses Postn, and re-enters the cell cycle. This specialized population is required for cardiac repair and scar formation after injury, but a similar population has not previously been reported in the developing heart. With more severe injuries, myofibroblasts, which are generated from activated Postn+ CFs and express αSMA, migrate to the injury area (15). Here, we report the presence of heterogeneous CF populations at P3 and P7 based on differential expression of endogenous *Postn* and *Tcf21* genes, but pathologic αSMA+ myofibroblasts were not observed during this critical period of ECM remodeling in the week after birth. There is some overlap between the Tcf21 and Postn-expressing CFs lineages at P7, but a separate population of *Tcf21*-negative Postn+ lineage cells also was observed at P7. Lineage tracing initiated before P7 demonstrates that the Postn+ CFs persist in the heart at P30, but they down-regulate endogenous *Postn* expression while expressing *Tcf21*. However, Postn+ lineage CFs are not detected with induction at P30, confirming the transient Postn expression and activation of this subpopulation. Gene expression profiling of Postn+P7, Tcf21+P7, and Tcf21+P30 sorted CFs demonstrates that the three populations share a fibroblastic gene profile, but also differentially express genes related to specific cellular functions. The Tcf21+ P30 CFs exhibit immune crosstalk functions, which has been reported in CF homeostasis and after injury (28). On the other hand, at P7, the Tcf21+ cells express genes related to ECM regulation, which is

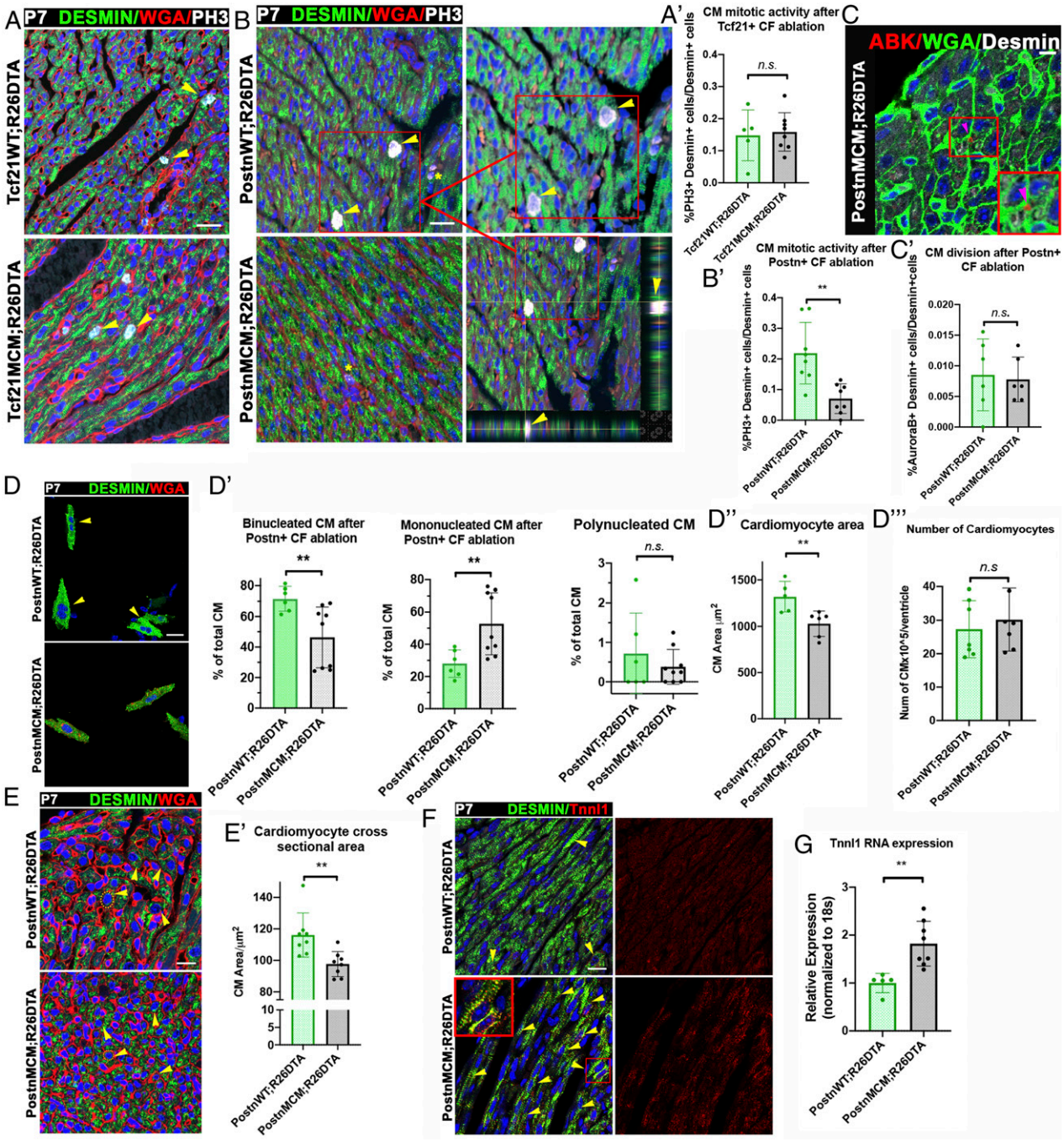

Fig. 6. The ablation of Postn+ CFs reduces cardiomyocyte mitotic activity and hypertrophic growth. (*A* and *B*) *Tcf21*^{MCM};*R26*^{DTA} and control *Tcf21*^{WT};*R26*^{DTA} and *Postn*^{MCM};*R26*^{DTA} and control *Postn*^{WT};*R26*^{DTA} Desmin/PH3 left ventricle immunostaining with WGA at P7. Z-stack 3D confocal images (borders) show Desmin surrounding the PH3+ nuclei confirming cardiomyocyte identity. Arrowheads show PH3+ CM in control hearts while the stars indicate a PH3+ CM after Postn+ CF ablation. (Scale bar: 10 µm.) (*A′* and *B′*) Quantification of *A* and *B* shows reduced cardiomyocyte mitotic activity after Postn+ but not after Tcf21+ CF ablation. $n = 5$ to 8. (*C*) P7 *Postn*^{MCM};*R26*^{DTA} left ventricle AuroraB Kinase and Desmin immunostaining with WGA. (Scale bar: 5 µm.) $n = 6$. (*C′*). Cytokinesis events in cardiomyocytes from *D* shows no effects of Postn+ CF ablation. $n = 6$. (*D*) Representative images of dissociated *Postn*^{MCM};*R26*^{DTA} and control *Postn*^{WT};*R26*^{DTA} cardiomyocytes (Desmin+ in green) at P7 shows decreased binucleation after Postn CF ablation. Arrowheads point to binucleated cardiomyocytes. DAPI was used to stain the nuclei. (*D′*) Percentage of binucleated, mononucleated, and polynucleated cardiomyocytes from *G*. There is a statistically significant reduction of binucleation after Postn+ CF ablation. $n = 6$ to 9. (*D″*) Quantification of the dissociated CM area. The CMs isolated from the Postn+ CF-ablated hearts are statistically significantly smaller. $n = 6$ to 9. An average of 100 CMs were measured per biological replicate. (*D‴*) Dissociated CM quantification per milligram of ventricular tissue. No differences in the number of CM were found after Postn+ CF ablation. $n = 7$. (*E*) *R26*^{DTA} and *Postn*^{MCM};*R26*^{DTA} and control *Postn*^{WT};*R26*^{DTA} left ventricle cross-sectional area of CMs indicated by Desmin immunostaining with WGA detection of cell boundaries at P7. (Scale bar: 10 µm.) (*E′*) Cross-sectional area measurement of cardiomyocytes from *C* shows reduced cardiomyocyte size after Postn+ CF ablation at P7. $n = 8$. An average of 50 CMs in cross section were measured per biological replicate. (*F*) P7 *Postn*^{MCM};*R26*^{DTA} and control *Postn*^{WT};*R26*^{DTA} left ventricle TnnI1 and Desmin immunostaining. Arrowheads point to cardiomyocytes with positive expression of TnnI1 (Scale bar: 5 µm.) $n = 6$. (*G*) RT-qPCR of *TnnI1* showed a statistically significant differences between *Postn*^{MCM};*R26*^{DTA} and *Postn*^{MCM};*R26*^{WT} at P7. $n = 5$ to 8. $^{**}P < 0.01$, $^{*}P < 0.05$, n.s., not significant by Mann–Whitney test.

considered the principal role of this cell type. In contrast, the Postn+ lineage CFs have enhanced cell-cycling gene expression, similar to adult reparative fibroblasts after injury (15, 16), and also neuronal growth signaling, which has not been previously reported. Recently, using single nuclei transcriptomics, two different neonatal populations of CFs in the postnatal heart have been described (29). Here, we demonstrate CF heterogeneity at P7 in vivo evident in specialized Postn+ and Tcf21+ CF populations with distinct functions in postnatal cardiac maturation.

The specialized Postn+ lineage CFs in the postnatal heart have shared characteristics with the reparative Postn+ CFs induced after cardiac injury in adult mice (14), including enhanced proliferation. Compared with adult Postn+ cells reported by Kanisicak et al. (14), the Postn+P7 CFs also have increased expression of *Fn*, *Col1* and *3*, *Adam12*, and *Wisp1*, but the higher levels of expression of *Egf*, *Igf2*, and neuron-growth–related genes are unique to postnatal Postn+P7 CFs. Hence, the Postn+ CFs at P7 share some, but not all, characteristics of the reparative activated Postn+ CFs present after adult injury. Both the Postn+P7 CFs and Tcf21+P7 CFs are also different from the pathologic activated myofibroblasts observed after injury, in that they do not express aSMA (8). While the Postn+ CFs are no longer detected with lineage tracing initiated at P30, the Tcf21+P30 CFs have decreased ECM gene expression and relatively increased complement gene expression similar to quiescent CFs in adults. Cell lineage analysis shows that Postn+ CFs repress endogenous Postn+ expression and become quiescent CFs at P30, but the ability of these specialized Postn-expressing CFs to preferentially reactivate after injury in comparison to other CFs is unknown. Together, these data demonstrate CF heterogeneity in the postnatal period, including the presence of a specialized population of CFs that express Postn transiently and share some properties with adult CFs involved in cardiac repair after injury.

Traditionally, neurons are known to communicate with the cells of the glia, but not much is known about their relationship with fibroblasts or roles in heart development. In vitro studies suggest a role for CFs in nerve development and synapse stability (30), but this has not been shown previously in vivo. In the neonatal heart, Postn+ P7 CFs are present in proximity to sympathetic nerves and express genes related to neuronal development, including secreted factors involved in neurogenesis. In addition, ablation of Postn+ CFs, but not Tcf21+ CFs, at P7 increased the neuronal surface area without significant changes in neuronal branching. The meaning of this increased nerve area remains unclear, but could represent an overgrowth of the cardiac nerves due to the lack of neuroregulators such as *Bdnf* (31) or *Nlgn1* (32) that are expressed by Postn+ CFs. Cardiac innervation is an important component of the conduction system in the heart; thus alterations in the normal ECG could be related to nerve abnormalities. With ablation of the Postn+ CFs at P7, ECG demonstrates a deeper Q wave, which is related to abnormal ventricular impulse transmission often related to myocardial infarction in humans, but how this extrapolates to mice is not clear. On the other hand, proper cardiac innervation is required for postnatal cardiac regeneration and CM proliferation (33). In addition to possible CF-nerve crosstalk, the alterations observed in the sympathetic nerves could be related to the cardiac glial cells, which were recently described as a population of cardiac stromal cells in single-cell RNAseq analysis (25). The proximity of Postn+ CFs to cells expressing Ngfr, a glial cell marker, further supports this interaction. Together, our in vivo findings provide initial evidence for communication of Postn+ CFs with nerves and/or glia in postnatal nerve maturation and patterning, but additional studies are needed to define potential crosstalk mechanisms and specific contributions to cardiac regenerative capacity or conduction maturation after birth.

Crosstalk between cardiomyocytes and fibroblasts has been described in vitro and related to cardiac injury and regeneration (34), but in vivo evidence in the postnatal heart and demonstration of the direct effect of CFs on cardiomyocyte maturation has not been described previously. Interestingly, Postn+ lineage CF ablation after birth leads to reduced cardiomyocyte mitotic activity and binucleation, as well as decreased CM size and increased presence of fetal troponin (TnnI1). Other markers of CM maturation remained unchanged after Postn+ CF ablation, which may reflect later maturation events. Together, these results support a direct function for Postn+ CFs in cardiomyocyte maturation and the switch to hypertrophic growth in the first week after birth. Strikingly, even with a reduction in CM size and no changes in the number of ventricular CMs, heart weight was not significantly different in the Postn-ablated hearts. The exact reason is unclear, but the changes in other cells or in the cardiomyocyte weight could be compensating. Also, it is remarkable that even with an impaired maturation of CM in the first week after birth, the ablated hearts do not present any functional abnormality at P30. This is suggestive of a compensatory growth phase after P7 that could be related to a reported peak of thyroid hormone at P21 (35). A possible additional function of these Postn+ CFs is in ECM remodeling, as Postn has been described to have a variety of effects on collagen both in vitro and in vivo (5). However, collagen remodeling and deposition were not altered with Postn+ lineage cell ablation at P7. While Postn protein expression is produced in the first week after birth, it is unlikely that the changes in CM maturation after Postn+ lineage cell ablation are exclusively related to reduced Postn presence since loss of Postn has no direct effect on CM cell-cycling activity (36). It is more likely that secreted factors from Postn+ cells affect CM mitotic activity and binucleation. Among the up-regulated ligands in the Postn+ CFs in agreement with a recent study (24) is *Igf2bp1*, which is increased in P7 compared to P30 CFs. Another Igf2-binding protein (*Igf2bp3*) has been recently related to cardiac regenerative capacity and CM proliferation at P1 to P8, but it was not clear which cells were producing it (24). Here we demonstrate that *Igf2bp1* is expressed more at P7 than at P30, specifically in CFs. Together, these findings implicate postnatal Postn+ CFs in the transition from hyperplasic to hypertrophic growth and in binucleation of CMs in the week after birth.

In summary, we have described the presence, expression, and function of different populations of postnatal CFs, finding a heterogeneous specialized population of Postn+ postnatal CFs that are active from P0 to P11 and transition to quiescence by P30. This specialized population has high proliferation rates and expression of nerve-related genes distinct from the more prevalent Tcf21+ lineage CFs. The ablation of the Postn+ P7 CFs reduces binucleation and hypertrophic growth in postnatal CMs, while also affecting surface nerve patterning in the ventricles. Thus, the Postn+ lineage CFs have critical effects on other cells, including nerves and CMs, in the early postnatal heart.

Materials and Methods

All experiments with mice were performed according to NIH guidelines, and all protocols involving animals were approved by the Cincinnati Children's Hospital Institutional Animal Care and Use Committee. Detailed information on the genetic lines used, protocols, and analytical methods can be found in *SI Appendix, SI Materials and Methods*. Five-micrometer paraffin sections and whole-mount hearts were used. The immunofluorescence protocols, RNAscope protocol, and a list of antibodies and probes can be found in *SI Appendix*. Cell death was detected by TUNEL staining using the In-Situ Cell Death Detection Kit from Roche. Collagen remodeling was detected using a fluorescently tagged Collagen Hybridizing Peptide (3Helix). A confocal Nikon Eclipse Ti Fluorescence microscope with NIS elements software (Nikon) was used for immunofluorescence imaging. Images were quantified automatically or manually using analysis NIS elements (Nikon). Whole-mount

imaging was performed on the upright FN1 microscope. A cross-sectional area of CMs was quantified manually in Fiji (37).

Data Availability. RNA-seq data have been deposited in the Gene Expression Omnibus database under accession number GSE144587. A detailed list of protocols can be found in *SI Appendix, SI Materials and Methods*. Raw data from this paper have been deposited at https://data.mendeley.com/datasets/yh98ftn3jy/2.

ACKNOWLEDGMENTS. We thank the confocal imaging core at Cincinnati Children's Hospital Medical Center (CCHMC) for helping with the whole-mount tissue processing and imaging. All flow cytometric data were acquired using equipment maintained by the Research Flow Cytometry Core in the Division of Rheumatology at CCHMC. We also thank all the counsel and advice received from Nathan Salomonis, Anne Katrine Johansen, and Hadi Khalil during the development of this work and acknowledge the help and support received from the Yutzey laboratory. Funding to support this work was provided by NIH Grant R01 HL142217 (to K.E.Y. and J.D.M.); a postdoctoral fellowship from the American Heart Association; the Lawrence J. and Florence A. DeGeorge Charitable Trust Grant #19POST34380004 (to L.H.); and a Postdoctoral Strauss Award from the CCHMC (to L.H.).

1. G. A. Roth *et al*., Global, regional, and national burden of cardiovascular diseases for 10 causes, 1990 to 2015. *J. Am. Coll. Cardiol.* **70**, 1–25 (2017).
2. F. Li, X. Wang, J. M. Capasso, A. M. Gerdes, Rapid transition of cardiac myocytes from hyperplasia to hypertrophy during postnatal development. *J. Mol. Cell. Cardiol.* **28**, 1737–1746 (1996).
3. S. Walsh, A. Pontén, B. K. Fleischmann, S. Jovinge, Cardiomyocyte cell cycle control and growth estimation in vivo: An analysis based on cardiomyocyte nuclei. *Cardiovasc. Res.* **86**, 365–373 (2010).
4. E. R. Porrello, E. N. Olson, A neonatal blueprint for cardiac regeneration. *Stem Cell Res.* **13**, 556–570 (2014).
5. L. Hortells, A. K. Z. Johansen, K. E. Yutzey, Cardiac fibroblasts and the extracellular matrix in regenerative and nonregenerative hearts. *J. Cardiovasc. Dev. Dis.* **6**, 29 (2019).
6. Y. Yahalom-Ronen, D. Rajchman, R. Sarig, B. Geiger, E. Tzahor, Reduced matrix rigidity promotes neonatal cardiomyocyte dedifferentiation, proliferation and clonal expansion. *eLife* **4**, e07455 (2015).
7. M. J. Ivey, M. D. Tallquist, Defining the cardiac fibroblast. *Circ. J.* **80**, 2269–2276 (2016).
8. M. D. Tallquist, J. D. Molkentin, Redefining the identity of cardiac fibroblasts. *Nat. Rev. Cardiol.* **14**, 484–491 (2017).
9. C. M. Braitsch, K. E. Yutzey, Transcriptional control of cell lineage development in epicardium-derived cells. *J. Dev. Biol.* **1**, 92–111 (2013).
10. P. Snider *et al*., Origin of cardiac fibroblasts and the role of periostin. *Circ. Res.* **105**, 934–947 (2009).
11. M. Ieda *et al*., Cardiac fibroblasts regulate myocardial proliferation through beta1 integrin signaling. *Dev. Cell* **16**, 233–244 (2009).
12. D. A. Skelly *et al*., Single-cell transcriptional profiling reveals cellular diversity and intercommunication in the mouse heart. *Cell Rep.* **22**, 600–610 (2018).
13. T. Oka *et al*., Genetic manipulation of periostin expression reveals a role in cardiac hypertrophy and ventricular remodeling. *Circ. Res.* **101**, 313–321 (2007).
14. O. Kanisicak *et al*., Genetic lineage tracing defines myofibroblast origin and function in the injured heart. *Nat. Commun.* **7**, 12260 (2016).
15. X. Fu *et al*., Specialized fibroblast differentiated states underlie scar formation in the infarcted mouse heart. *J. Clin. Invest.* **128**, 2127–2143 (2018).
16. H. Kaur *et al*., Targeted ablation of periostin-expressing activated fibroblasts prevents adverse cardiac remodeling in mice. *Circ. Res.* **118**, 1906–1917 (2016).
17. M. Hesse, A. Welz, B. K. Fleischmann, Heart regeneration and the cardiomyocyte cell cycle. *Pflugers Arch.* **470**, 241–248 (2018).
18. M. H. Soonpaa, K. K. Kim, L. Pajak, M. Franklin, L. J. Field, Cardiomyocyte DNA synthesis and binucleation during murine development. *Am. J. Physiol.* **271**, H2183–H2189 (1996).
19. Z. Yin, J. Ren, W. Guo, Sarcomeric protein isoform transitions in cardiac muscle: A journey to heart failure. *Biochim. Biophys. Acta* **1852**, 47–52 (2015).
20. G. D. Lopaschuk, J. S. Jaswal, Energy metabolic phenotype of the cardiomyocyte during development, differentiation, and postnatal maturation. *J. Cardiovasc. Pharmacol.* **56**, 130–140 (2010).
21. M. Horackova, J. Slavikova, Z. Byczko, Postnatal development of the rat intrinsic cardiac nervous system: A confocal laser scanning microscopy study in whole-mount atria. *Tissue Cell* **32**, 377–388 (2000).
22. C. Williams, K. P. Quinn, I. Georgakoudi, L. D. Black III, Young developmental age cardiac extracellular matrix promotes the expansion of neonatal cardiomyocytes in vitro. *Acta Biomater.* **10**, 194–204 (2014).
23. P. Rodriguez *et al*., Deletion of delta-like 1 homologue accelerates fibroblast-myofibroblast differentiation and induces myocardial fibrosis. *Eur. Heart J.* **40**, 967–978 (2019).
24. Z. Wang *et al*., Mechanistic basis of neonatal heart regeneration revealed by transcriptome and histone modification profiling. *Proc. Natl. Acad. Sci. U.S.A.* **116**, 18455–18465 (2019).
25. N. Farbehi *et al*., Single-cell expression profiling reveals dynamic flux of cardiac stromal, vascular and immune cells in health and injury. *eLife* **8**, e43882 (2019).
26. S. Majkut, P. C. Dingal, D. E. Discher, Stress sensitivity and mechanotransduction during heart development. *Curr. Biol.* **24**, R495–R501 (2014).
27. N. Velayutham *et al*., Cardiomyocyte cell cycling, maturation, and growth by multinucleation in postnatal swine. *J. Mol. Cell. Cardiol.* **146**, 95–108, 10.1016/j.yjmcc.2020.07.004 (2020).
28. S. Van Linthout, K. Miteva, C. Tschöpe, Crosstalk between fibroblasts and inflammatory cells. *Cardiovasc. Res.* **102**, 258–269 (2014).
29. P. Hu *et al*., Single-nucleus transcriptomic survey of cell diversity and functional maturation in postnatal mammalian hearts. *Genes Dev.* **32**, 1344–1357 (2018).
30. C. Mias *et al*., Cardiac fibroblasts regulate sympathetic nerve sprouting and neurocardiac synapse stability. *PLoS One* **8**, e79068 (2013).
31. E. Pius-Sadowska, B. Machaliński, BDNF: A key player in cardiovascular system. *J. Mol. Cell. Cardiol.* **110**, 54–60 (2017).
32. P. Scheiffele, J. Fan, J. Choih, R. Fetter, T. Serafini, Neuroligin expressed in nonneuronal cells triggers presynaptic development in contacting axons. *Cell* **101**, 657–669 (2000).
33. A. I. Mahmoud *et al*., Nerves regulate cardiomyocyte proliferation and heart regeneration. *Dev. Cell* **34**, 387–399 (2015).
34. J. E. Cartledge *et al*., Functional crosstalk between cardiac fibroblasts and adult cardiomyocytes by soluble mediators. *Cardiovasc. Res.* **105**, 260–270 (2015).
35. M. Li *et al*., Thyroid hormone action in postnatal heart development. *Stem Cell Res.* **13**, 582–591 (2014).
36. A. Lorts, J. A. Schwanekamp, J. W. Elrod, M. A. Sargent, J. D. Molkentin, Genetic manipulation of periostin expression in the heart does not affect myocyte content, cell cycle activity, or cardiac repair. *Circ. Res.* **104**, e1–e7 (2009).
37. J. Schindelin *et al*., Fiji: An open-source platform for biological-image analysis. *Nat. Methods* **9**, 676–682 (2012).